Endocrine remodelling of the adult intestine sustains reproduction in *Drosophila*

Tobias Reiff[1,*], Jake Jacobson[2,*], Paola Cognigni[2,6,*], Zeus Antonello[1,*], Esther Ballesta[1], Kah Junn Tan[4], Joanne Y. Yew[3,4,5], Maria Dominguez[1,7], Irene Miguel-Aliaga[2,7]

[1] Instituto de Neurociencias, Consejo Superior de Investigaciones Cientificas - Universidad Miguel Hernández (CSIC-UMH), Sant Joan d'Alacant, Alicante, 03550, Spain.
[2] MRC Clinical Sciences Centre, Imperial College London, Hammersmith Campus, Du Cane Road, London W12 0NN, UK.
[3] Temasek Life Sciences Laboratory, 1 Research Link, Singapore 117604.
[4] Department of Biological Sciences, National University of Singapore, 14 Science Drive 4, Singapore 117543.
[5] Pacific Biosciences Research Center, University of Hawai'i at Mānoa, Honolulu, HI 96822, USA.
[6] Current address: Centre for Neural Circuits and Behaviour, The University of Oxford, Mansfield Road, Oxford OX1 3SR, UK.
[7] Co-corresponding authors.
[*] Equal contribution, reverse alphabetical order.

Authors for correspondence:

M.D.	m.dominguez@umh.es	Phone + 34 965919390
I.M-A.	i.miguel-aliaga@imperial.ac.uk	Phone +44 (0)2083833907

Running title: Intestinal remodelling sustains reproduction

Abstract

The production of offspring is energetically costly and relies on incompletely understood mechanisms that generate a positive energy balance. In mothers of many species, changes in key energy-associated internal organs are common yet poorly characterized functionally and mechanistically. Here we show that, in adult *Drosophila* females, the midgut is dramatically remodelled to enhance reproductive output. In contrast to extant models, organ remodelling does not occur in response to increased nutrient intake and/or offspring demands, but rather precedes them. With spatially and temporally directed manipulations, we identify juvenile hormone as an anticipatory endocrine signal released after mating. Acting through intestinal bHLH-PAS domain proteins Met and Gce, JH signals directly to intestinal progenitors to yield a larger organ, and adjusts gene expression and SREBP activity in enterocytes to support increased lipid metabolism. Our findings identify a metabolically significant paradigm of adult somatic organ remodelling linking hormonal signals, epithelial plasticity and reproductive output.

Introduction

Reproduction is energetically costly. Mothers can adjust their energy balance to maximise their reproductive success through well-established neural mechanisms that match food intake to their enhanced energy requirements (Roa and Tena-Sempere, 2014). However, less understood changes also occur in many animals during reproduction; internal organs, such as the liver, pancreas and gastrointestinal tract, increase their size and adapt their physiology, potentially contributing to an increased generation and delivery of nutrients (Hammond, 1997; Speakman, 2008).

Establishment of a positive energy balance may be particularly important to animals with a reproductive strategy that involves rapid production of large numbers of progeny. *Drosophila melanogaster* females can lay up to 100 eggs per day at the peak of their fertility in early life (David et al., 1974; Klepsatel et al., 2013). We hypothesised that such demands may rely on large regulatory responses, which are amenable to genetic investigation in this model system. A network of organs and tissues in *Drosophila* perform many of the same basic functions as those found in mammals (Padmanabha and Baker, 2014), so we sought to explore the nature and significance of organ plasticity during reproduction.

Results

The *Drosophila* adult midgut is remodelled in female flies after mating

Female flies actively engaged in reproduction undergo multiple adaptations including changes in digestive physiology (Cognigni et al., 2011). This prompted us to character ise possible intestinal changes occurring during the phase of peak fertility (David et al., 1974; Klepsatel et al., 2013). We focused on the midgut epithelium because of its major digestive/absorptive roles (Lemaitre and Miguel-Aliaga, 2013). In the midgut epithelium, long-lived progenitors (intestinal stem cells) divide to self-renew and to give rise to committed progenitors (called enteroblasts), which directly differentiate into two types of progeny: absorptive enterocytes and enteroendocrine cells (Jiang and Edgar, 2012). We found that mating transiently increases the number of both dividing and differentiating midgut cells, as revealed by phospho-Histone H3 (pH3) stainings and temporal analyses of progenitors and their descendants using the dual labelling system *escargot*-Repressible Dual Differential Marker (*esgReDDM*, Antonello et al., in press) (Figures 1A, 1C and 1E). The midgut of mated females also becomes visibly larger; gut diameter measurements

were suggestive of a net increase in the number of postmitotic intestinal cells (Figures 1B and 1D, Figure 1 – supplement 1): an increase that we confirmed by cell number and density counts (Figure 1F, Figure 1 – supplement 1). Concurrent with midgut re-sizing, we observed mating-dependent activation of the single *Drosophila* homologue of the mammalian family of sterol regulatory element binding proteins (SREBP (Seegmiller et al., 2002; Shimano, 2001; Theopold et al., 1996), also known as *HLH106* in flies, Figures 2A and 2B), using a reporter subject to the same physiologically-regulated proteolytic processing as wild-type SREBP (Kunte et al., 2006). SREBP activation after mating was accompanied by upregulation of midgut transcripts involved in fatty acid synthesis and activation (*SREBP*, the long-chain fatty acid CoA ligases *bubblegum* (*bgm*) and *Acyl-CoA synthetase long-chain* (*Acsl*) and, depending on genetic background, *Fatty acid synthase* (*FAS*) and *Acetyl-CoA carboxylase* (*ACC*) (Figures 2E-2F), many of which are known SREBP targets in flies and/or mammals (Horton et al., 2003; Seegmiller et al., 2002). Immunohistochemical analyses using reporters pointed to the enterocytes located in the posterior midgut region (R5, Buchon et al., 2013; Marianes and Spradling, 2013) as preferential sites of transcriptional and SREBP activity changes (Figures 2A-2D). Thus, in female flies actively engaged in reproduction, changes in both intestinal progenitors and their progeny parallel those observed in mammals leading to hyperplasia (Hammond, 1997; Speakman, 2008), increased organ size (Hammond, 1997; Speakman, 2008) and upregulation of lipid gene expression (Athippozhy et al., 2011).

Intestinal remodelling is mediated by increased levels of circulating juvenile hormone

Female flies change their physiology and behaviour (e.g. by increasing egg production and food intake) in response to male-derived peptides acquired during mating (Barnes et al., 2008; Carvalho et al., 2006). The synthesis of juvenile hormone (JH) in the *corpus allatum*, an endocrine gland, can be stimulated *ex vivo* by the male-derived sex peptide, suggesting regulation by mating (Moshitzky et al., 1996). Using rapid direct analysis in real time (DART) mass spectrometry, we profiled haemolymph of both virgin and mated female flies and established that the levels of *in vivo* circulating JH are indeed increased after mating (Figure 3A). The levels of two other juvenoid compounds, JH3-bisepoxide (JH3B) and methylfarnesoate (MF), were too low to be detected. We cannot, however, rule out that they also are regulated by mating and contribute to signalling through the JH pathway (Tiu et al., 2012; Wen et al., 2015; Yin et al., 1995). JH has been shown to sustain ovarian maturation through pleiotropic actions on adipose and reproductive tissues (Flatt et al., 2005), but its intestinal roles remain to be established. Consistent with a possible

intestinal role, we detected transcript upregulation of the JH target *Kruppel homolog 1* (*Kr-h1*) (Jindra et al., 2013) in guts of mated females (Figure 3 – supplement 1). To explore the roles of JH signalling on intestinal remodelling, we first fed methoprene, a JH analogue (JHa) (Cerf and Georghiou, 1972), to virgin female flies. This led to effects on intestinal progenitors, gut diameter and lipid metabolism comparable to those triggered by mating (Figures 3B-3E, 3H, Figure 3 – supplement 1). We next blocked endogenous JH production by mis-expressing the protein phosphatase inhibitor *NiPp1* using the *corpus allatum*-specific driver *Aug21-Gal4* (Siegmund and Korge, 2001): a genetic manipulation known to result in adult-specific ablation of the *corpus allatum* and a dramatic reduction of JH titers in the haemolymph (Yamamoto et al., 2013). Depletion of systemic JH prevented mating-triggered remodelling: a phenotype that could be restored in these gland-ablated flies by JHa feeding (Figures 3F and 3I).

Juvenile hormone signals directly to adult intestinal progenitors and enterocytes via Met and Gce receptors

To establish the cellular targets of JH and its mode of action, we interfered with JH signalling in a cell-autonomous manner in the intestine. We used the *esgReDDM* system, based on the widely used *esg-Gal4* driver (Micchelli and Perrimon, 2006), to target both classes of intestinal progenitor cells (intestinal stem cells and enteroblasts). We first confirmed that expression of RNAi transgenes against either of the two previously identified JH receptors *Methoprene-tolerant* (*Met*) or *germ cell-expressed bHLH-PAS* (*gce*) (Jindra et al., 2013) resulted in a significant reduction in their transcript levels (Figure 3 – supplement 1). We then confined expression of these RNAi transgenes against *Met*, *gce*, or their target *Kr-h1* to adult intestinal progenitors using *esgReDDM*. Downregulation of any of these three genes fully prevented both the proliferative response to mating and midgut re-sizing, whereas overexpression of *Kr-h1* lead to mating-like responses in virgin females (Figures 3G and 3J, Figure 3 – supplement 1), indicating direct actions of JH on intestinal progenitors. Intestinal progenitors with downregulated JH receptors were found in numbers comparable to those of controls in virgin females, and were able to increase their proliferation in response to a JH-unrelated stimulus: the ROS-inducing compound paraquat (Biteau et al., 2008) (Figure 3 – supplement 1). This indicates that they remain competent to respond to the well-studied homeostatic machinery that maintains gut integrity (Jiang and Edgar, 2012), and suggests that mating- and damage-induced proliferative mechanisms may differ and can be uncoupled. In enterocytes, targeted by the specific driver *Mex-Gal4* (Phillips and Thomas, 2006), only downregulation of *gce*

strongly reduced the mating-dependent upregulation of a *bgm* reporter (Figures 3K, Figure 3 – supplement 1). Together, these findings show that intestinal remodelling results from a rise in systemic JH triggered by mating. JH signals directly to intestinal progenitors to yield a larger organ in a *Met* and *gce*-dependent manner. Acting predominantly through *gce*, JH also adjusts gene expression in enterocytes to support increased lipid metabolism.

Mating-triggered intestinal remodelling enhances reproductive output

Intestinal remodelling during reproduction could result from increased nutrient intake (O'Brien et al., 2011) or utilisation by the developing offspring. Alternatively, it may occur in preparation for, but be uncoupled from, such nutritional demands. Consistent with the latter idea, the mating-triggered changes in proliferation, midgut size and SREBP activity are all still apparent in sterile female ovo^{D1} mutant flies, in which egg production is blocked prior to vitellogenesis and which do not increase food intake after mating (Barnes et al., 2008) (Figure 4 – supplement 1). To investigate the significance of intestinal remodelling, we used several RNAi transgenes to downregulate either the JH receptor *gce* or *SREBP*, which is activated by mating, specifically in adult enterocytes. In all cases, enterocyte-specific downregulation led to a reduction in the number (but not viability) of eggs produced (Figure 4E, 4F and Figure 4 – supplement 1), indicating that JH signalling is required to specifically enhance the quantity (fecundity), but not the quality (viability), of reproductive output. Progenitor cell-specific downregulation may also be expected to reduce fecundity; however, we detected expression of the *esg-Gal4* driver in the stem cell niche of the ovary (data not shown), which could lead to direct effects on egg production independently of the intestine. More specific tools will be necessary to resolve this important issue.

The anatomical proximity between the ovary and the posterior midgut region where changes in lipid gene expression and activity take place (Figures 4A and 4D) raises the intriguing possibility that enhanced nutrient delivery from the intestine to the ovary may occur locally, to maximise loading into eggs. As the trafficked nutrients would be therefore released in the form of eggs, we used sterile ovo^{D1} females to quantify lipid content, reasoning that it might accumulate in gut and/or peripheral fat stores in the absence of the local ovarian sink (Parra-Peralbo and Culi, 2011). Consistent with this idea, sterile ovo^{D1} female flies accumulate peripheral fat after mating (Figures 4B and 4C), and lipid accumulation in the posterior midgut could be induced in fertile flies by either treatment of these sterile flies with JHa or by knocking down lipid shuttling proteins acutely, thereby blocking all lipid circulation (Palm et al., 2012) (Figures 4G-4J). Together,

these data show that the metabolic reprogramming of enterocytes by JH supports fecundity, thus confirming that intestinal plasticity is required to sustain reproductive output at the time of peak fertility. The importance of intestinal lipogenesis is becoming increasingly recognized in both flies and mammals (Lodhi et al., 2011; Palm et al., 2012; Sieber and Thummel, 2012; Song et al., 2014), and here we show that it underpins reproductive output. Notably, upregulation of *SREBP* target genes has been reported in the small intestine of lactating rats (Athippozhy et al., 2011), suggesting that our findings may be conserved beyond insects.

Discussion

Intestinal remodelling and the costs of reproduction

The onset of reproduction involves a significant shift in metabolic demands, now routed towards the growing offspring as well as the mother. *Drosophila* may experience a particularly extreme example of this shift when a young female is mated: an event which enhances egg production tenfold and triggers multiple metabolic and behavioural adaptations (Avila et al., 2011; Cognigni et al., 2011; Kubli, 2003; Rogina et al., 2007). These changes are in large part brought about by signals delivered by the male during copulation, in particular the Sex Peptide (Avila et al., 2011; Kubli, 2003). Several reports connect SP to the *corpus allatum* and JH production (Bontonou et al., 2015; Moshitzky et al., 1996), suggesting that the systemic effects of mating via SP could be carried out through this pathway. Intriguingly, both JH knockdown in females (Yamamoto et al., 2013) and SP deficiency in males (Wigby and Chapman, 2005) extend female lifespan while reducing reproductive output and/or peak fertility. This “cost of mating” on lifespan is not relieved by sterility (Ueyama and Fuyama, 2003), suggesting that physiological effects in non-reproductive tissues are responsible. The intestinal reprogramming that we describe here represents a novel physiological target of postmating plasticity ideally placed at the interface between nutrition and reproduction. Aging in flies is accompanied by reduced fertility (Economos et al., 1979) and intestinal dysplasia (Biteau et al., 2008; Choi et al., 2008), and genetic manipulations that affect intestinal progenitors can affect lifespan (Biteau et al., 2010; Rera et al., 2011). Thus, it will be informative to explore the links between JH-triggered postmating responses in lifespan, age-dependent intestinal and reproductive dysfunction, and lifetime fertility.

Hormonal remodelling of adult organs

In the larva, the *corpora allata* integrate age and metabolic status information to optimise developmental progression (Mirth and Shingleton, 2012; Sarraf-Zadeh et al., 2013). Increasing evidence is revealing that, in adults, this insect endocrine organ acts as a nexus that detects changes in the organism's circumstances and condition to alter its metabolic and/or reproductive set points. It does so through regulated release of JH, with pleiotropic effects on ovarian maturation, adipose tissue, learning and memory, diapause, innate immunity and ageing (Fahrbach and Robinson, 1996; Flatt et al., 2005; Jowett and Postlethwait, 1980; Nijhout and Riddiford, 1974; Riddiford, 2012; Wyatt and Davey, 1996; Yamamoto et al., 2013). Some of these effects may be modulated by crosstalk between JH and other systemic signals such as insulin-like peptides and ecdysteroids (Jindra et al., 2013; Koyama et al., 2013; Mirth et al., 2014; Rauschenbach et al., 2014), but the cellular and molecular targets of JH action remain incompletely understood. Our findings have uncovered a direct and functionally significant effect on adult organ plasticity by showing that JH promotes proliferation and resets gut size through its actions on intestinal progenitors, and activates expression of lipid metabolism genes in enterocytes. Based on structural and functional similarities, insect JH has been compared to mammalian thyroid hormones (Flatt et al., 2006): key energy balance regulators often associated with gastrointestinal alterations when pathologically dysregulated (Middleton, 1971). Given the well-established changes in thyroid function during human pregnancy (Glinoer, 1997), it will therefore be of interest to explore their contribution to reproductive intestinal remodelling. Downstream of its receptor(s), relay of JH signalling in the intestine may differ from the classical model in which *Met* and *gce* act redundantly (Abdou et al., 2011; Jindra et al., 2013). Indeed, downregulation of either gene alone is sufficient to prevent the mating-induced changes in intestinal progenitors: a finding that we confirmed by observing that viable Met^{27} mutants also fail to undergo mating-induced remodelling (data not shown). The actions of Met and Gce may also be cell-specific, as suggested by a preferential requirement for *gce* in enterocytes, and may result from different Met/gce expression levels (our unpublished observations) and/or interacting partners. Candidates to consider include Taiman, homolohous to the mammalian steroid receptor coactivator 1 (SRC-1)/NCoA-1/p160 (Charles et al., 2011; Li et al., 2011; Zhang et al., 2011) and, more intriguingly, circadian clock proteins: Met-binding partners recently shown to coordinate the switch from diapause to reproduction in other insects (Bajgar et al., 2013; Shin et al., 2012).

Adult organ plasticity, obesity and cancer

Adult organ plasticity is not a peculiarity of *Drosophila* reproduction; examples of changes in intestinal size and nutrient utilization are widespread across the animal kingdom in response to both environmental and internal challenges (Carey, 1990; Hammond, 1997; O'Brien et al., 2011; Piersma and Lindstrom, 1997; Speakman, 2008). Although intestinal remodelling has not been assessed in human pregnancy, it could be one of the major drivers for the changes in gut microbiota observed during pregnancy (Koren et al., 2012) and could contribute to changes in gastrointestinal physiology, common during pregnancy (Keller et al., 2008). Resetting of anatomical or metabolic features of internal organs may thus be a broadly used strategy to achieve a positive energy balance which, when matched to the developing offspring's demands, will contribute to reproductive success. However, if deployed in the absence of such demands, organ remodelling could contribute to the weight gain and increased fat mass that has been observed upon gonadectomy of multiple species including mice, rats, cats, monkeys, and other mammals (Hansen et al., 2013 and references therein). In a more physiological context, inappropriate persistence of such metabolic remodelling beyond pregnancy and lactation could similarly contribute to post-pregnancy weight retention in humans - a phenotype that, at least in mice, is correlated with enhanced intestinal function (Casirola and Ferraris, 2003; Gore et al., 2003). Similarly, inappropriate persistence of juvenile hormone-like mechanisms that change the homeostatic set point of adult stem cells and their progeny to transform an organ may also help explain why pregnancy changes the susceptibility to certain cancers (Gwinn et al., 1990).

Acknowledgements

We thank Antoine Ducuing for his assistance with the initial SREBP experiments, and Suzanne Eaton and Wilhelm Palm for sharing lipid transport data and reagents prior to publication. We are grateful to Frederic Bernard, Edward Dubrowsky, Suzanne Eaton, Marek Jindra, Christen Mirth, Isabel Palacios, Julien Royet, Alex Shingleton and Graham Thomas for reagents. We also Thomas Carroll for statistical advice and Dafni Hadjieconomou, Bruno Hudry, Bryn Owen, Esmeralda Parra-Peralbo, Daniel Perea and Marc Tatar for comments on the manuscript. This work was funded by grants from the Wellcome Trust, European Research Council and the Medical Research Council (WT083559, ERCStG 310411 and intramural to IM-A), Generalitat Valenciana (PROMETEO II/2013/001 to MD), Spanish Ministry of Science (BFU2009-09074, SAF2012-35181,

CSD2007-00023 to MD), Botin Foundation (to MD) and the Singapore National Research Foundation (RF2010-06 to JYY). TR held a postdoctoral fellowship from the Deutsche Forschungsgemeinschaft and IM-A is a member of, and is supported by, the EMBO Young Investigator Programme.

Figure Legends

Figure 1. Mating increases intestinal stem cell proliferation and gut size. (**A**, **A**') Using the *esgReDDM* tracer (Antonello et al., in press), intestinal progenitors (intestinal stem cells and enteroblasts) are labelled with GFP and RFP, whereas the postmitotic progeny (enterocytes and enteroendocrine cells) that these progenitors give rise to in a defined time window is labelled with RFP only (see Supplemental Information for additional details). At 3 days after mating, the posterior midgut of mated flies contains more newly generated postmitotic progeny (**A**) compared to age-matched virgins (**A'**). It has also become visibly larger (**B** and **B'**). At this time point, these guts also have a higher number of nuclei marked by the mitotic marker pH3 in both w^{1118} and OregonR backgrounds (**C**, $p = 0.008$, and **E**, $p < 0.001$, negative binomial GLM), although the proliferation increase is transient (data not shown). The size increase is quantified in the posterior midgut by measuring midgut diameter (**D**, $p < 0.001$, t-test) and counting the number of cells labelled by the enterocyte marker *caudal-Gal4* (**F**, $p = 0.02$, t-test). See Table 1 for full genotypes.

Figure 1 – figure supplement 1. Mating re-sizes the *Drosophila* gut. The increase in gut size at 3 days after mating is also measurable (**A**, **A'**) and significant (**B**, $p < 0.001$, t-test) in the OregonR background. The *esgReDDM* tracing system reveals that mated guts contain more cells generated in the last 7 days if the fly had been mated in that time (**C**, $p < 0.001$, t-test) than if it had not. The size increase is not due to stretching of the tissue, as the density of nuclei in the posterior midgut remains the same (**D**, $p = 0.77$, t-test). See Table 1 for full genotypes.

Figure 2. Mating activates a transcriptional lipogenic program in the intestine. At 3 days after mating, increased expression of a reporter transgene that replicates the transcriptional regulation and post-translational modification of SREBP is apparent in the posterior midgut (**A**, **A'**, quantified in **B**, $p < 0.001$, Mann-Whitney test). A *bgm* transcriptional reporter is also increased specifically in the enterocytes of the posterior

midgut following mating (**C**, **C'**, quantified in **D**, p = 0.002, Mann-Whitney test). Transcript abundance of *SREBP*, *bgm* and the *SREBP* targets *Acsl*, *FAS* and *ACC* is increased by mating in either one or both of the w^{1118} and OregonR backgrounds (**E** w^{1118}: p = 0.02 *SREBP*, p = 0.02 *bgm*, p = 0.005 *Acsl*, p = 0.5 *FAS*, p = 0.3 *ACC*; **F** OregonR: p = 0.02 *SREBP*, p = 0.03 *bgm*, p = 0.03 *Acsl*, p = 0.01 *FAS*, p = 0.04 *ACC*, paired one-tailed t-test). See Table 1 for full genotypes.

Figure 3. Systemic JH secreted after mating acts directly in the intestinal epithelium to drive reproductive remodelling. Circulating JH is elevated after mating in the haemolymph of female flies (**A**, p = 0.02 at 24 h, p = 0.002 at 48 h, t-test with Holm's correction). Increased tissue renewal (**B**, **B'**) and SREBP activation (**C**, **C'**, quantified in **D**, p < 0.001, Mann-Whitney test) are apparent following a 3-day dietary supplementation with JHa. JHa treatment is sufficient to increase mitoses (**E**, p < 0.001, negative binomial GLM) and size (**H**, p < 0.001, t-test) of the posterior midgut. Conversely, when the endogenous JH source is genetically ablated by means of *Aug21 > NiPp1* (Yamamoto et al., 2013), the proliferation and size increase that follow mating are abolished, although they can be reinstated by feeding JHa (proliferation **F**, p < 0.001 between *Aug21 / +* and *Aug21 > NiPp1* mated, p < 0.001 between *Aug21 > NiPp1* and *NiPp1 / +* mated, p < 0.001 between *Aug21 > NiPp1* and *Aug21 > NiPp1* + JHa mated; all relevant comparisons between virgins are not significant, negative binomial GLM with Holm's correction; gut diameter **i**, p = 0.002 between *Aug21 / +* and *Aug21 > NiPp1* mated, p < 0.001 between *Aug21 > NiPp1* and *NiPp1 / +* mated, p < 0.001 between *Aug21 > NiPp1* and *Aug21 > NiPp1* + JHa mated; all relevant comparisons between virgins are not significant, t-test with Holm's correction). Downregulation of either *gce* or *Met* in adult progenitors abrogates post-mating proliferation (**G**, p < 0.001 between *esgReDDM / +* and *esgReDDM > gce RNAi* mated, p < 0.001 between *esgReDDM / +* and *esgReDDM > Met RNAi* mated, negative binomial GLM with Holm's correction) and gut size increase (**J**, p < 0.001 between *esgReDDM / +* and *esgReDDM > gce RNAi* mated, p < 0.001 between *esgReDDM / +* and *esgReDDM > Met RNAi* mated, t-test with Holm's correction). The upregulation of *bgm* reporter upon mating is abolished by the downregulation of *gce*, but not *Met*, in enterocytes using the enterocyte-specific driver *Mex-Gal4* (**K-K''''**). See Table 1 for full genotypes.

Figure 3 – figure supplement 1. Intestinal JH signalling is relayed through Kr-h1 and underlies mating-dependent intestinal growth and gene expression phenotypes. JHa application in virgin females results in a net growth of the gut, as shown by the increase in

caudal-marked cells (**A**, p = 0.004, t-test). The JH signalling pathway can be targeted using RNAi constructs against the receptors *Met* and *gce*, which decrease transcript abundance compared to a tub^{TS} control when expressed globally in larvae for 3 hours at 29°C (**B**, p = 0.002 for *Met*, p = 0.005 for *gce*, paired one-tailed t-test). Consequently, using *esgReDDM* to specifically knock down *gce* in adult intestinal progenitor cells abolishes the proliferative effect of JHa application (**C**, **C'**), but does not reduce the number of progenitors after 7 days of downregulation (**D**, p > 0.05, t test). Progenitors in which *gce* is downregulated can still proliferate normally to replenish a gut damaged by a 24 h application of the toxin paraquat (**E**, **E'** with quantification of mitoses in **F**, p < 0.001 for both *esgReDDM / +* and *esgReDDM > gce RNAi*, p > 0.05 for all other relevant comparisons, t test with Holm's correction) and the number of progenitors is not reduced by this treatment (**G**, p = 0.04 between *esgReDDM / +* untreated control and *esgReDDM > gce RNAi* untreated control, p > 0.05 for all other relevant comparisons, t test with Holm's correction). The transcription factor *Kruppel homolog 1* (*Kr-h1*), a well-established effector of JH responses, is transcriptionally upregulated after 3 days of mating (**H**, p = 0.02 in w^{1118}, p = 0.02 in OregonR, paired two-tailed t-test). *Kr-h1* function is necessary and sufficient for the re-sizing of the gut after mating, as its downregulation in intestinal progenitors through RNA interference using *esgReDDM* prevents the increase in proliferation (**I**, p < 0.001 between *esgReDDM / +* and *esgReDDM > Kr-h1 RNAi* mated, negative binomial GLM with Holm's correction) and gut size (**J**, p < 0.001 between *esgReDDM / +* and *esgReDDM > Kr-h1 RNAi* mated, t-test with Holm's correction) typically observed after 7 days of mating, while overexpression of *Kr-h1* constructs from the same cells recapitulates the effect of mating in virgins (proliferation, **I**, p < 0.001 between *esgReDDM / +* and *esgReDDM > Kr-h1*$_{GS}$ virgin, p < 0.001 between *esgReDDM / +* and *esgReDDM > Kr-h1*$_{UAS}$ virgin, negative binomial GLM with Holm's correction; gut size **J**, p < 0.001 between *esgReDDM / +* and *esgReDDM > Kr-h1*$_{UAS}$ virgin, t-test with Holm's correction). RNAi constructs against *Kr-h1* and *SREBP* are effective in downregulating these genes; they decrease transcript abundance compared to a tub^{TS} control when expressed globally in larvae for 3 hours at 29°C (**K**, p = 0.02 for *Kr-H1*, p < 0.001 for both *SREBP* constructs, paired one-tailed t-test). Downregulating *gce* constitutively from enterocytes using *Mex-Gal4* significantly suppresses the transcriptional increase of the lipid metabolism gene *bgm* upon mating, as indicated by the intensity ranking of a *gce* reporter (**L**, p = 0.004 between *gce RNAi / +* and *Mex > gce RNAi*, p = 0.02 between *Mex > gce RNAi* and *Mex / KK control*, Mann-Whitney test with Holm's correction; relevant comparisons with *Met RNAi* are not significant). See Table 1 for full genotypes.

Figure 4. Metabolic remodelling of enterocytes by JH sustains reproduction. Lipid-harbouring tissues (fat body, posterior midgut and ovary) are found in close proximity in the fly's abdomen (represented schematically in **A**, and in confocal microscopy in **D**). The amount of stored triglycerides (TAG) in the carcass of 3-day mated sterile female flies is increased compared to virgins (**B**, p = 0.003 in w^{1118}, p = 0.009 in OregonR, t-test), as quantified by thin-layer chromatography (**C**). Adult-specific downregulation of JH receptors *gce* and *Met* or *SREBP* in enterocytes reduces the total progeny produced by females in the 6 days following their first mating (**E**, p = 0.01 between *Met RNAi / +* and Mex^{TS} *> Met RNAi*, p = 0.007 between Mex^{TS} *> Met RNAi* and Mex^{TS} */ KK* control, p < 0.001 between *gce RNAi / +* and Mex^{TS} *> gce RNAi*, p = 0.007 between Mex^{TS} *> gce RNAi* and Mex^{TS} */ KK* control; **F** p = 0.04 between *SREBP RNAi / +* and Mex^{TS} *> SREBP RNAi*, p = 0.04 between Mex^{TS} *> SREBP RNAi* and Mex^{TS} */ TRiP* control, t-test with Holm's correction). In the absence of the ovarian lipid sink in sterile ovo^{D1} virgin flies, treatment with JHa increases neutral lipid content, as revealed by Oil Red O staining, in the posterior midgut (**G**, **G'**, quantified in **H**: p = 0.002, t-test). Acute block of lipid export by heat-shock activation of *lpp >stop> LTP RNAi* (Palm et al., 2012) in virgin females results in heavy accumulation of neutral lipid in this gut region, further indicating that this midgut region provides a net source of lipid in adult flies (**I**, quantified in **J**: p < 0.001 between *LTP RNAi / +* and *lpp >stop> LTP RNAi*, p < 0.001 between *lpp >stop> LTP RNAi* and *lpp >stop> / +*, p < 0.001 between *lpp >stop> LTP RNAi* and *lpp >stop> LTP RNAi* heat shock control, t-test with Holm's correction). See Table 1 for full genotypes.

Figure 4 – figure supplement 1. Reproductive intestinal remodelling is uncoupled from germline demands and is needed to sustain reproduction. Sterile females carrying the ovo^{D1} mutation experience the post-mating increase in progenitor proliferation (**A**, p < 0.001 for w^{1118} and ovo^{D1}, negative binomial GLM, visualised in **C** and **C'** using the *esgReDDM* tracing system), gut size increase (**B**, p < 0.001 for w^{1118} and ovo^{D1}, t-test), and *SREBP* reporter activation (**D**, p < 0.001 for w^{1118} and p = 0.005 for ovo^{D1}, Mann-Whitney test, visualised in **E** and **E'**). The role of intestinal remodelling in enhancing reproductive capacity is confirmed with additional RNA interference lines against the JH receptor *gce* (chosen because of its larger effect in Fig. 4E; **F**, p = 0.002 between *GD11178 / +* and Mex^{TS} *> GD11178*, p = 0.008 between Mex^{TS} *> GD11178* and Mex^{TS} */ +*, p < 0.001 between *GD47465 / +* and Mex^{TS} *> GD47465*, p = 0.003 between Mex^{TS} *> GD11178* and Mex^{TS} */ +*, t-test with Holm's correction) and *SREBP* (**G**, p = 0.008 between *GD37641 / +* and Mex^{TS} *>*

GD37641, p < 0.001 between *GD37640 / +* and *Mex^{TS} > GD37640*, t-test). Despite these effect on fecundity, eggs laid by *gce*, *Met* or *SREBP* RNAi mothers are viable (**H** and **I**, mean hatched fraction > 0.9 for all groups, p > 0.05 for all relevant comparisons, t-test). See Table 1 for full genotypes.

Genotype in text/figure	**Full genotype**	**Figure panel(s)**
esgReDDM	*w ; esg-Gal4 , UAS-CD8::GFP / + ; tub-Gal80^{TS} , UAS-H2B::RFP / + ; +*	1A S1C S1D 3B
w^{1118} background	*w^{1118} ; + ; + ; +*	1B 1C 1D 2E 3E 3H S3H S4A S4B
OregonR background	*+ ; + ; + ; +*	1E S1A S1B 2F S3H
caudal > H2B::RFP	*w ; caudal-Gal4 /+; UAS H2B::RFP /+ ; +*	1F S3A
SREBP > CD8::GFP	*w / + ; SREBP-Gal4 / + ; UAS-CD8::GFP / + ; +*	2A 2B 3C 3D 4D S4D
bgm-lacZ	*w / + ; bgm-lacZ / + ; + ; +*	2C 2D
CantonS background	*+ ; + ; + ; +*	3A
Aug21 / +	*w ; Aug21-Gal4 / + ; + ; +*	3F 3I
Aug21 > NiPp1	*w ; Aug21-Gal4 / + ; UAS-NiPp1 / + ; +*	3F 3I
NiPp1 / +	*w ; + ; UAS-NiPp1 / + ; +*	3F 3I
esgReDDM / +	*w ; esg-Gal4 , UAS-CD8::GFP / + ; tub-Gal80^{TS} , UAS-H2B::RFP / + ; +*	3G 3J S3D S3F S3G S3I S3J
esgReDDM > gce RNAi	*w ; esg-Gal4 , UAS-CD8::GFP / UAS-gce RNAi KK101814 ; tub-Gal80^{TS} , UAS-H2B::RFP / + ; +*	3G 3J S3C S3D S3E S3F S3G
esgReDDM > Met RNAi	*w ; esg-Gal4 , UAS-CD8::GFP / UAS-Met RNAi KK100638 ; tub-Gal80^{TS} , UAS-H2B::RFP / + ; +*	3G 3J
esgReDDM > Kr-h1 RNAi	*w ; esg-Gal4 , UAS-CD8::GFP / UAS-Kr-h1 RNAi KK107935 ; tub-Gal80^{TS} , UAS-H2B::RFP / + ; +*	S3I S3J
esgReDDM > Kr-h1$_{GS}$	*w ; esg-Gal4 , UAS-CD8::GFP / UAS-Kr-h1$_{GS}$; tub-Gal80^{TS} , UAS-H2B::RFP / + ; +*	S3I
esgReDDM > Kr-h1$_{UAS}$	*w ; esg-Gal4 , UAS-CD8::GFP / UAS-Kr-h1$_{UAS}$; tub-Gal80^{TS} , UAS-H2B::RFP / + ; +*	S3I S3J
tub^{TS} > Met RNAi	*w ; tub-Gal80^{TS} / UAS-Met RNAi KK100638 ; tub-Gal4 , UAS-CD8::GFP / + ; +*	S3B
tub^{TS} > gce RNAi	*w ; tub-Gal80^{TS} / UAS-gce RNAi KK101814 ; tub-Gal4 , UAS-CD8::GFP / + ; +*	S3B
tub^{TS} > Kr-h1 RNAi	*w ; tub-Gal80^{TS} / UAS-Kr-h1 RNAi KK107935 ; tub-Gal4 , UAS-CD8::GFP / + ; +*	S3K
tub^{TS} > SREBP RNAi GD	*w ; tub-Gal80^{TS} / UAS- SREBP RNAi GD37640 ; tub-Gal4 , UAS-CD8::GFP / + ; +*	S3K
tub^{TS} > SREBP RNAi TRiP	*w ; tub-Gal80^{TS} / + ; tub-Gal4 , UAS-CD8::GFP / UAS- SREBP RNAi TRiP34073 ; +*	S3K
tub^{TS} / +	*w ; tub-Gal80^{TS} / + ; tub-Gal4 , UAS-CD8::GFP / + ; +*	S3B S3K (control)
Met RNAi / +	*w ; bgm-lacZ / UAS-Met RNAi KK100638 ; + ; +*	3K S3L
Mex > Met RNAi	*w ; Mex-Gal4 , bgm-lacZ / UAS-Met RNAi KK100638 ; + ; +*	3K S3L
gce RNAi / +	*w ; bgm-lacZ / UAS-gce RNAi KK101814 ; + ; +*	3K S3L
Mex > gce RNAi	*w ; Mex-Gal4 , bgm-lacZ / UAS-gce RNAi KK101814 ; + ; +*	3K S3L
Mex / KK control	*w ; Mex-Gal4 , bgm-lacZ / attp40 ; + ; +*	3K S3L
ovo^{D1} (*w^{1118}* background)	*w^{1118} ; + ; ovo^{D1} / + ; +*	4C S4A S4B
ovo^{D1} (OregonR background)	*+ / w^{1118} ; + ; ovo^{D1} / + ; +*	4C 4G 4H
Met RNAi / +	*w ; UAS-Met RNAi KK100638 / + ; + ; +*	4E S4H

Mex^{TS} > Met RNAi	*w ; Mex-Gal4 / UAS-Met RNAi KK100638; tub-Gal80TS / + ; +*	4E S4H
gce RNAi / +	*w ; UAS-gce RNAi KK101814 / + ; + ; +*	4E S4H
Mex^{TS} > gce RNAi	*w ; Mex-Gal4 / UAS-gce RNAi KK101814 ; tub-Gal80TS / + ; +*	4E S4H
Mex^{TS} / KK control	*w ; Mex-Gal4 / attp40 ; tub-Gal80TS / + ; +*	4E S4H
SREBP RNAi / +	*w / y , v ; + ; UAS-SREBP RNAi 34073 ; +*	4F
Mex^{TS} > SREBP RNAi	*w / y , v ; Mex-Gal4 / + ; tub-Gal80TS / SREBP RNAi 34073 ; +*	4F
Mex^{TS} / TRiP control	*w / y , v ; Mex-Gal4 / + ; tub-Gal80TS / UAS-GFP ; +*	4F
hs-FLP lpp >stop> LTP RNAi	*w , hs-FLP / w ; lpp-Gal4 / + ; UAS >stop> LTP RNAi / + ; +*	4I 4J
UAS >stop> LTP RNAi / +	*w ; + ; UAS >stop> LTP RNAi / + ; +*	4J
hs-FLP lpp / +	*w , hs-FLP / w ; lpp-Gal4 / + ; + ; +*	4J
esgReDDM / ovo^{D1}	*ovo^{D1} / w ; esg-Gal4 , UAS-CD8::GFP / + ; tub-Gal80^{TS} , UAS-H2B::RFP / + ; +*	S4C
SREBP > CD8::GFP / ovo^{D1}	*w / + ; SREBP-Gal4 / + ; UAS-CD8::GFP / ovoD1 ; +*	S4D S4E
gce RNAi GD11178 / +	*w ; UAS-gce RNAi GD11178 ; + ; +*	S4F
Mex^{TS} >gce RNAi GD11178	*w ; Mex-Gal4 / UAS-gce RNAi GD11178 ; tub-Gal80^{TS} / + ; +*	S4F
gce RNAi GD47465 / +	*w ; + ; UAS-gce RNAi GD47465 / + ; +*	S4F
Mex^{TS} > gce RNAi GD47465	*w ; Mex-Gal4 / + ; tub-Gal80^{TS} / UAS-gce RNAi GD47465 ; +*	S4F
Mex^{TS} / +	*w ; Mex-Gal4 / + ; tub-Gal80^{TS} / + ; +*	S4F
SREBP RNAi GD37641 / +	*w ; UAS-SREBP RNAi GD37641 / + ; + ; +*	S4G S4I
Mex^{TS} > GD37641	*w ; Mex-Gal4 / UAS-SREBP RNAi GD37641 ; tub-Gal80^{TS} / + ; +*	S4G S4I
SREBP RNAi GD37640 / +	*w ; UAS-SREBP RNAi GD37640 / + ; +*	S4G S4I
Mex^{TS} > RNAi GD37640	*w ; Mex-Gal4 / + ; tub-Gal80^{TS} / UAS-SREBP RNAi GD37640 ; +*	S4G S4I

Table 1. Full genotypes. S1 denotes Figure 1 – supplement 1; S3 denotes Figure 3 – supplement 1; S4 denotes Figure 4 – supplement 1.

Experimental Procedures

Fly strains

For wild-type experiments, the genetic backgrounds *w^{1118}*, OregonR and CantonS were used as indicated in the figures and/or full genotypes list (Table 1). The following transgenic and mutant stocks were used: *esg-Gal4* (Bloomington, unknown insertion), *tub-Gal80^{TS}* (Bloomington 7018, McGuire et al., 2003), *UAS-CD8::GFP* (Bloomington 5130, Lee and Luo, 1999), *UAS-H2B::RFP* (presumed from Langevin et al., 2005), *caudal-Gal4* (insertion used in Ryu et al., 2008), *SREBP-Gal4* (Bloomington 38395, Kunte et al., 2006), *bgm-lacZ* (Bloomington 28120, Min and Benzer, 1999), *Aug21-Gal4* (Bloomington 30137, Siegmund and Korge, 2001), *UAS-NiPp1* (Bloomington 23712, Parker et al., 2002), *tub-Gal4* (Bloomington 5138, Lee and Luo, 1999), *Mex-Gal4* (Phillips and Thomas, 2006), *UAS-Kr-h1* (DGRC 120052, referred to as *UAS-Kr-h1$_{UAS}$*), *ovo^{D1}* (Busson et al., 1983), *hs-FLP ; lpp-Gal4* and *UAS >stop> LTP RNAi* stocks (both from Palm et al., 2012). RNAi constructs were obtained from VDRC for *gce* (KK101814, GD11178 and GD47465), *Met* (KK100638), *Kr-h1*

(KK107935) and *SREBP* (GD37641 and GD37640), as well as the genetically matched KK control (KK60100); and from the Bloomington TRiP collection for *SREBP* (34073) and the genetically matched TRiP control (GFP in valium10, 35786). Because the control stocks are generated in the same background as the *RNAi* lines used, the *Gal4* parental control (e.g. *yv ; Mex-Gal4 / + ; tubGa80^{ts} / UAS-GFP*) are genetically matched to the experimental genotype (e.g. *yv ; Mex-Gal4 / + ; tubGal80^{ts} / UAS-SREBP RNAi TRiP*). The line referred to as *UAS-Kr-h1$_{GS}$* is *GS(2)73ES2b*, which was isolated in a genetic screen for enhancer/suppressors of a large eye phenotype caused by Dl overexpression in the Dominguez lab. Genomic DNA flanking the P-element insertions in the *GS(2)73ES2b* stock were recovered by inverse PCR and sequenced. A BLAST search with the obtained sequence produced perfect matches to the genomic region upstream of the *Kr-h1* gene (26B5 Chromosome 2L:6,082,603..6,096,498).

Fly husbandry

Fly stocks were reared on a standard cornmeal/agar diet (5.5% cornmeal, 6% dextrose, 1.3% yeast, 0.55% agar supplemented with 0.18% nipagin and 2.9 mL/L propionic acid) or 'Iberian' diet (4.4% wheat flour, 6% brown sugar, 3% yeast, 1% agar supplemented with 0.04% nipagin and 7.6 mL/L of propionic acid). All experimental flies were kept at 25^{o} C expect for those containing temperature-sensitive regulation (*tub-Gal80^{TS}*) which were set up at 18^{o}C (restrictive temperature) and transferred to 29^{o}C (permissive temperature) at the time when activation was needed in the specific experiment. For all experiments, experimental and control flies were handled in parallel and experienced the same temperature shifts and treatments.

For the analysis of mating and juvenile hormone analogue (JHa) effects, virgin female flies were collected at eclosion, aged for 4-5 days on standard food and then transferred for 3 days (7 days for flies harbouring the *esgReDDM* transgenes, as these flies shows a delay in mating responses at 29^{o}C) into new tubes in the presence of wild-type males (typically 4-5 females + 6 males) or food supplemented with 1.5 mM methoprene (Sigma PESTANAL 33375, racemic mixture, added to freshly prepared food when still liquid but < 50^{o}C. This concentration was chosen in a pilot dilution test from 0.5 to 7.5 mM as the one which induced activation of the *SREBP-Gal4* reporter to levels comparable to mating, and corresponds to approximately half of the concentration used in a previous study (Flatt and Kawecki, 2007). Controls were age-matched virgin females which were also transferred to new tubes for the same time but without the addition of males and/or methoprene.

For the paraquat experiments, virgin female flies were raised at 18°C and aged for 4-5 days after eclosion, at which point they were starved for 4 hours without water. The flies were then transferred to vials containing filter paper soaked in 5% sucrose with or without 10mM paraquat dichloride (Sigma Aldrich). After spending 24 hours at 29^{o}C in these vials, their midguts were dissected and stained for pH3 as described before.

Antibodies

The following antibodies were used: rabbit anti-pH3 (1:2000, Upstate), sheep anti-GFP (1:1000, Biogenesis, for *esgReDDM* staining), goat anti-GFP (1:1500, Abcam, for *SREBP > CD8::GFP* staining), rabbit anti-β-galactosidase (1:5000, MP biomedicals); secondary antibodies were either FITC/Cy3 conjugates from Jackson Immunolabs (1:200, for *SREBP > CD8::GFP* and *bgm-lacZ*) or Alexa488/647 conjugates from Invitrogen (1:1000, for *esgReDDM* and *caudal > H2B::RFP*). Preparations for proliferation analysis were counterstained with DAPI (Sigma) and mounted in Fluoromount-G (Southern Biotech). Preparations for reporter analysis were mounted in Vectashield with DAPI (Vectorlabs).

Proliferation and size quantifications

Quantification of mitoses in wild-type and *ovo^{D1}* female flies was carried out by counting individual nuclei marked by the mitotic marker pH3 using a Nikon Eclipse 90i Fluorescence microscope through a 40x objective. For the acquisition of gut images in these samples, a single 1392x1040 field was acquired posterior to the midgut-hindgut boundary using QCapture software (QImaging). Progeny dynamics were analysed using the *esgReDDM* system (Antonello et al., in press), which has the genetic makeup *esg-Gal4, UAS-CD8::GFP; tub-Gal80^{TS}, UAS-H2B::RFP*. At the permissive temperature of 29^{o}C, the GFP reporter is expressed in *esg-Gal4* positive cells (intestinal stem cells, ISCs, and enteroblasts, EBs), but due to the perdurance of the RFP-tagged histone *H2B::RFP*, red additionally marks the *esg-Gal4*-negative progeny (including enterocytes, ECs, and enteroendocrine cells, EECs) generated from these progenitors since the shift to permissive temperature. To restrict progeny analysis to mating-induced changes, *esgReDDM* flies were maintained at 18^{o}C, such that Gal4 expression is suppressed by *tub Gal80^{TS}*, and moved to 29^{o}C only at the time of mating. After 3 days of mating at 29^{o}C, guts were dissected and stained for GFP and pH3 (the endogenous RFP signal was detected directly). Enterocyte number in the posterior midgut was assessed by imaging the entire gut of *caudal > H2B::RFP* flies and counting the number of RFP-marked cells. Confocal images were obtained with a Leica TCS SP5 inverted confocal microscope using a 20x air objective for *esgReDDM* and a 10x air

objective for *caudal > H2B::RFP*. Stacks were typically collected every 1 µm and the images (1024x1024) were reconstructed using maximum projection. Bright field images or confocal maximum projections were loaded into ImageJ (Schneider et al., 2012) and the line tool used to quantify the width of the gut across the centre of the image. ImageJ was also used to outline the guts of *esgReDDM* flies using the polygon tool before analysing the resulting region of interest (ROI) with a custom MATLAB (The MathWorks, Inc.) script optimized for the ReDDM method. Extended details about this analysis are available from (Antonello et al., in press). Briefly, maximum projections were adjusted for levels and offsets and filtered to remove noise (using always the same parameters for scans within one experiment), then the area of the gut was identified by background staining and the cell nuclei by DAPI signal. The size of nuclei can be used to discriminate between diploid cells (intestinal stem cells (ISCs), enteroblasts (EBs), and enteroendocrine cells (EECs)) and polyploid enterocytes (ECs). The red-labelled nuclei (persistent H2B::RFP) and green-labelled cells (CD8::GFP expression) were identified by segmentation and compared to the pattern of nuclei defined by DAPI to generate a report of total ECs (large DAPI cells), total progenitors + progeny (RFP signal), total ISCs and EBs (GFP signal), and total area. The same script was also used to count the number of *caudal > H2B::RFP* cells.

Analysis of reporter gene expression

For *SREBP > CD8::GFP* and *bgm-lacZ* experiments, confocal images were obtained with a Leica SP5 upright confocal microscope using a 20x glycerol immersion objective. A single 20x field (1024 pixels wide) immediately posterior to the midgut-hindgut boundary was acquired with a Z resolution of 1.5 µm. ImageJ was used to generate a maximum projection for each sample and all images pertaining to one experiment were loaded as separate layers into a single Adobe Photoshop CS6 file. The layers were then ranked blindly on the basis of their relative intensity in the relevant channel.

qPCR

To quantify mating-induced changes in gene expression, posterior midguts from at least 10 adult female flies were dissected, dissecting out Malphigian tubules and the hindgut. To determine the knockdown efficiency of the RNAi transgenes, *tubGal80^{TS}; tubGal4,UASGFP* was used to downregulate them ubiquitously. 8-10 third-instar larvae were collected from crosses kept at 21°C, and were shifted to 29°C for three hours to allow RNAi transgene expression. Samples (posterior midguts or whole larvae) were directly stored on dry ice and at -80 °C in RNAlater TissueProtect Tubes (Qiagen) until total

RNA was extracted using RNeasy Mini Kit (Qiagen), from which cDNAs were prepared with SuperScript First-Strand Synthesis System (Invitrogen) using oligo-dT primers. Quantitative PCR was performed using the SYBR Green PCR Master Mix (Applied Biosystems) in a 7500 Real-Time PCR System (Applied Biosystems) using *rp49* as a housekeeping control gene. All qPCRs were performed in triplicate and the relative expression was calculated using comparative Ct method.
Primers used:

	forward 5`-3`	*reverse 3`-5`*
SREBP	GCAAAGTGCGTTGACATTAACC	AGTGTCGTGTCCATTGCGAA
bgm	GCAATCGATTTGCGTGACCA	GGCCCAGGACGATTGTAGAG
Acsl	CGGAGATCCGACAAAGCAGT	TGAGCACAGCTCCTCAAAGG
FAS	GACATTCGATCGACGCCTCT	GCTTTGGCTTCTGCACTGAC
ACC	AATTCTCCAAGGCTCGTCCC	CATGCCGCAATTGTTTTCGC
Kr-h1	ACAATTTTATGATTCAGCCACAACC	GTTAGTGGAGGCGGAACCTG
gce	AGCTGCGTATCCTGGACACT	TCGAGAGCTGAAACATCTCCAT
Met	CCGCCGTCCTTAGATTCGC	GTTCCCTTGAGGCCGGTTT
Rp49	TGTCCTTCCAGCTTCAAGATGACCATC	CTTGGGCTTGCGCCATTTGTG

Detection of circulating JH hormone by DART-MS

Haemolymph was extracted from virgin or mated females using pulled glass microcapillary needles (10 µL volume, #2-000-010; Drummond Scientific, PA, USA). The needle tip was placed into the gap between the anepisternum and anepimeron of anesthetized flies and haemolymph was collected using a slight vacuum (0.2 -1.0 mPa) for ~30 s. Haemolymph from 45-50 flies were collected in the same needle. The contents were ejected into a 0.1 mL glass vial insert (Thermo Fisher Scientific, MA, USA) by applying pressurized air (~5-6 kPa) with a Femtojet microinjector (Eppendorf, NY, USA), and weighed prior to extraction. 20 µL of MeOH were added to the haemolymph followed by extraction with 20 µL of hexane, repeated 4 times. Pooled hexane extract was evaporated under a gentle stream of N_2 and reconstituted in 10 µL of hexane. All extracts were prepared and measured immediately after collection.

Mass spectra were acquired with an atmospheric pressure ionization time-of-flight mass spectrometer (AccuTOF-DART™, JEOL USA, Inc.) equipped with a DART interface and operated in negative-ion mode at a resolving power of 6000 (FWHM definition). The RF

ion guide voltage was set at 600 V. The atmospheric pressure ionization interface potentials were as follows: orifice 1 = 15 V, orifice 2 = 5 V, ring lens = 5 V. Mass spectra were stored at a rate of one spectrum per second with an acquired m/z range of 60-1000. The DART interface was operated in positive-ion mode using helium gas with the gas heater set to 200 °C. The glow discharge needle potential was set to 3.5 kV. Electrode 1 was set to +150 V and electrode 2 was set to +250 V. Helium gas flow was set to 2.0 L/min. Calibration for exact mass measurements was accomplished by acquiring a mass spectrum of polyethylene glycol (average molecular weight 600) as a reference standard in every data file. Analysis was done with JEOL MassCenter software (version 1.3.0.1). Accurate mass measures and isotope pattern matching by MassMountaineer (FarHawk Marketing Services, Ontario, CA) were used to support elemental composition assignments.

2 µL of the haemolymph hexane extract were placed on the tip of a borosilicate glass capillary. The capillary was introduced to the DART ion source with a micromanipulator, thus allowing for reproducible placement of the sample. Each extract was measured 4-5 times. The averaged signal intensity was normalized to the total weight of the haemolymph and converted to absolute quantities after establishing a calibration curve with a JHIII standard (Santa Cruz Biotechnology, CA, USA, CAS 24198-95-6). Analysis of JHIII by DART produces two signature ions at m/z 267.20 (intact molecule) and at m/z 249.18 (loss of water), consistent with a previous study (Navare et al., 2010). The abundance of the $[M\text{-}H_2O+H]^+$ signal peak was used for all measurements because the parent ion at m/z 267.20 could not be consistently resolved due to interference from other signals. To detect other juvenoid compounds, the following mass signatures were used: methyl farnesoate ($[M+H]^+$ 251.20) and JHIII Bisepoxide ($[M+H]^+$ 283.19). DART MS was previously shown to be an effective method for quantitative and high sensitivity measurements of JHIII (Navare et al., 2010).

Fecundity and egg viability experiments

Flies for fecundity and egg viability experiments were raised at 18^{o}C to prevent the expression of the RNAi transgenes during development, then shifted to 29^{o}C in late pupariation (after ~ 20 days). Virgin females were collected upon eclosion and after 4 days mated overnight to OregonR males (10 males, 10 females per vial). Males were then removed, individual female flies were transferred to a new single vial of yeast-supplemented standard food (cornmeal/agar diet with 5% yeast content) every 48 h and eggs were counted from the vacated vial to quantify fecundity. To assess egg viability, a fraction of the egg-containing vials were then maintained at 29^{o}C and the number of

eclosed progeny were counted and compared with egg counts. Each genotype cross was performed 3 times and egg production from each fly was assessed over 3 48 h repeats, covering a total of 6 days of egg laying.

Thin-layer chromatography (TLC)

Ovaries and guts were removed from flies immobilised on ice and the remaining carcasses (3 flies per sample) were immediately homogenised in a mixture of methanol (60 µl), chloroform (150 µl) and water (75 µL), following previously described procedures (Al-Anzi et al., 2009; Hildebrandt et al., 2011). After an extraction period (1 h at 37^{o}C), aqueous and organic phases were separated by the addition of a 1:1 mixture of 1 M potassium chloride and chloroform (75 µL each). Samples were briefly centrifuged and 120 µL of the organic phase was transferred to fresh Eppendorf tubes and left to air-dry for 3 h. The resulting dessicated lipids were resuspended in 16 µL of a 1:1 chloroform:methanol mixture. 3 µL of each sample was applied to thin layer chromatography plates (Merck 116487) and lipid species were separated by standing the plates in ~ 1 cm of a mobile phase consisting of 69.5% hexane, 29.5% diethyl ether and 1% acetic acid. Once the mobile phase had traversed the plates they were briefly dried and then dipped in a cerium-ammonium-molybdate stain (ammonium heptamolybdate tetrahydrate 2.5 g, cerium (IV) sulfate hydrate complex with sulphuric acid 1 g, water 90 mL, sulphuric acid 10 mL). The TLC plates were developed at 80^{o}C for 25 minutes and then imaged on a digital scanner. The TAG content was quantified by analysing the resulting TIFF images using the densitometry tool in ImageJ software. All reagents were purchased from Sigma.

Lipid export block

The shuttling of lipids between organs was abolished by downregulating the apolipoprotein lipid transfer protein (LTP) through heat-shock-activated acute RNAi expression based on the pFRiPE system (Marois and Eaton, 2007). In the larva, this manipulation prevents the loading of gut-originated medium-chain diacylglycerides, which are a dominant component of circulating lipids, onto the haemolymph carrier Lipophorin (Lpp) and leads to the accumulation of stored lipid in the larval gut in triglyceride form (Palm et al., 2012). The downregulation of *LTP* from the fat body driver *Lpp-Gal4* was triggered in virgin females by 1 h heat-shock at 37^{o}C; after 6 h, the guts were dissected for neutral lipid detection using Oil Red O staining.

Oil Red O stainings

Fly guts were dissected from flies immobilised on ice and were then fixed in a solution of 4% formaldehyde for 45 minutes. Guts were washed in consecutive applications of PBS, double-distilled water and a 60% isopropanol solution. Oil Red O (Sigma) stock was prepared as a 0.1% solution in isopropanol, then a freshly prepared working solution (a 6:4 dilution in water) was added for 20 minutes to the guts, then washed in 60% isopropanol and water. The preparations were mounted in glycerol for analysis and the posterior midgut was imaged using either a Zeiss Axioplan stereo microscope equipped with Nomarski optics or an Olympus BX53 phase contrast microscope equipped with a 4x / 0.13 UPlanFLN lens through CellSens software (Olympus). The resulting TIFF files were analysed quantitatively using a custom ImageJ script: the gut was manually outlined as a ROI using the polygon tool, then the RGB channels were split and the red channel subtracted from the green to eliminate background (grey) signal. The mean intensity of the resulting signal within the ROI was calculated with the built-in Analyse Particles function.

Statistics and figure preparation

All statistical analyses were carried out in the R environment (R Development Core Team, 2014). Comparisons between normally distributed groups were carried out using Student's t-test (R function t.test), unpaired, two-tailed and incorporating Welch's correction to account for unequal variances, followed by Bonferroni-Holm correction when multiple comparisons were applied. qPCR data were analysed comparing the housekeeping-subtracted Cts of experimentally matched virgin and mated samples, thus using paired t-test, one-tailed when confirming previous reporter experiments (Figures 2E and 2F) and two-tailed when no prediction could be made (panel H in Figure 3 – supplement 1). Count data with a distinctly non-normal distribution (specifically, pH3 counts) were fitted with a negative binomial model (R function glm.nb from MASS package, Venables and Ripley, 2002) followed by likelihood ratio tests (R function anova.negbin from MASS package). Rank-based experiments were analysed with the Mann-Whitney-Wilcoxon rank sum test (R function wilcox.test). All graphs were generated in R using a custom script based on the base boxplot function superimposed with individual data points plotted with the beeswarm function (package beeswarm). Confocal and bright field images shown in conjunction were always acquired with the same settings as part of a single experiment. For visualisation purposes, level and channel adjustments were applied using Adobe Photoshop CS6 to the confocal images shown in figure panels

(the same correction in all comparable images) but all quantitative analyses were carried out on unadjusted raw images or maximum projections.

References

Abdou, M.A., He, Q., Wen, D., Zyaan, O., Wang, J., Xu, J., Baumann, A.A., Joseph, J., Wilson, T.G., Li, S., and Wang, J. (2011). Drosophila Met and Gce are partially redundant in transducing juvenile hormone action. Insect biochemistry and molecular biology 41, 938-945.

Al-Anzi, B., Sapin, V., Waters, C., Zinn, K., Wyman, R.J., and Benzer, S. (2009). Obesity-blocking neurons in Drosophila. Neuron 63, 329-341.

Antonello, Z.A., Reiff, T., Ballesta, E., and Dominguez, M. Robust intestinal homeostasis relies on cellular plasticity in enteroblasts mediated by miR-8-Escargot switch. EMBO Journal, in press.

Athippozhy, A., Huang, L., Wooton-Kee, C.R., Zhao, T., Jungsuwadee, P., Stromberg, A.J., and Vore, M. (2011). Differential gene expression in liver and small intestine from lactating rats compared to age-matched virgin controls detects increased mRNA of cholesterol biosynthetic genes. BMC genomics 12, 95.

Avila, F.W., Sirot, L.K., LaFlamme, B.A., Rubinstein, C.D., and Wolfner, M.F. (2011). Insect seminal fluid proteins: identification and function. Annual review of entomology 56, 21-40.

Bajgar, A., Jindra, M., and Dolezel, D. (2013). Autonomous regulation of the insect gut by circadian genes acting downstream of juvenile hormone signaling. Proceedings of the National Academy of Sciences of the United States of America 110, 4416-4421.

Barnes, A.I., Wigby, S., Boone, J.M., Partridge, L., and Chapman, T. (2008). Feeding, fecundity and lifespan in female Drosophila melanogaster. Proceedings. Biological sciences / The Royal Society 275, 1675-1683.

Biteau, B., Hochmuth, C.E., and Jasper, H. (2008). JNK activity in somatic stem cells causes loss of tissue homeostasis in the aging Drosophila gut. Cell stem cell 3, 442-455.

Biteau, B., Karpac, J., Supoyo, S., Degennaro, M., Lehmann, R., and Jasper, H. (2010). Lifespan extension by preserving proliferative homeostasis in Drosophila. PLoS genetics 6, e1001159.

Bontonou, G., Shaik, H.A., Denis, B., and Wicker-Thomas, C. (2015). Acp70A regulates Drosophila pheromones through juvenile hormone induction. Insect biochemistry and molecular biology 56, 36-49.

Buchon, N., Osman, D., David, F.P., Fang, H.Y., Boquete, J.P., Deplancke, B., and Lemaitre, B. (2013). Morphological and molecular characterization of adult midgut compartmentalization in Drosophila. Cell reports 3, 1725-1738.

Busson, D., Gans, M., Komitopoulou, K., and Masson, M. (1983). Genetic Analysis of Three Dominant Female-Sterile Mutations Located on the X Chromosome of DROSOPHILA MELANOGASTER. Genetics 105, 309-325.

Carey, H.V. (1990). Seasonal changes in mucosal structure and function in ground squirrel intestine. The American journal of physiology 259, R385-392.

Carvalho, G.B., Kapahi, P., Anderson, D.J., and Benzer, S. (2006). Allocrine modulation of feeding behavior by the Sex Peptide of Drosophila. Current biology : CB 16, 692-696.

Casirola, D.M., and Ferraris, R.P. (2003). Role of the small intestine in postpartum weight retention in mice. The American journal of clinical nutrition 78, 1178-1187.

Cerf, D.C., and Georghiou, G.P. (1972). Evidence of cross-resistance to a juvenile hormone analogue in some insecticide-resistant houseflies. Nature 239, 401-402.

Charles, J.P., Iwema, T., Epa, V.C., Takaki, K., Rynes, J., and Jindra, M. (2011). Ligand-binding properties of a juvenile hormone receptor, Methoprene-tolerant. Proceedings of the National Academy of Sciences of the United States of America 108, 21128-21133.

Choi, N.H., Kim, J.G., Yang, D.J., Kim, Y.S., and Yoo, M.A. (2008). Age-related changes in Drosophila midgut are associated with PVF2, a PDGF/VEGF-like growth factor. Aging cell 7, 318-334.

Cognigni, P., Bailey, A.P., and Miguel-Aliaga, I. (2011). Enteric neurons and systemic signals couple nutritional and reproductive status with intestinal homeostasis. Cell metabolism 13, 92-104.

David, J., Biemont, C., and Fouillet, P. (1974). Sur la forme des courbes de ponte de Drosophila melanogaster et leur adjustement a des modeles mathematiques. Arch Zool Exp Gen 115, 263-267.

Economos, A.C., Miquel, J., Binnard, R., and Kessler, S. (1979). Quantitative analysis of mating behavior in aging male Drosophila melanogaster. Mechanisms of ageing and development 10, 233-240.

Fahrbach, S.E., and Robinson, G.E. (1996). Juvenile hormone, behavioral maturation, and brain structure in the honey bee. Developmental neuroscience 18, 102-114.

Flatt, T., and Kawecki, T.J. (2007). Juvenile hormone as a regulator of the trade-off between reproduction and life span in Drosophila melanogaster. Evolution; international journal of organic evolution 61, 1980-1991.

Flatt, T., Moroz, L.L., Tatar, M., and Heyland, A. (2006). Comparing thyroid and insect hormone signaling. Integrative and comparative biology 46, 777-794.

Flatt, T., Tu, M.P., and Tatar, M. (2005). Hormonal pleiotropy and the juvenile hormone regulation of Drosophila development and life history. BioEssays : news and reviews in molecular, cellular and developmental biology 27, 999-1010.

Glinoer, D. (1997). The regulation of thyroid function in pregnancy: pathways of endocrine adaptation from physiology to pathology. Endocrine reviews 18, 404-433.

Gore, S.A., Brown, D.M., and West, D.S. (2003). The role of postpartum weight retention in obesity among women: a review of the evidence. Annals of behavioral medicine : a publication of the Society of Behavioral Medicine 26, 149-159.

Gwinn, M.L., Lee, N.C., Rhodes, P.H., Layde, P.M., and Rubin, G.L. (1990). Pregnancy, breast feeding, and oral contraceptives and the risk of epithelial ovarian cancer. Journal of clinical epidemiology 43, 559-568.

Hammond, K.A. (1997). Adaptation of the maternal intestine during lactation. Journal of mammary gland biology and neoplasia 2, 243-252.

Hansen, M., Flatt, T., and Aguilaniu, H. (2013). Reproduction, fat metabolism, and life span: what is the connection? Cell metabolism 17, 10-19.

Hildebrandt, A., Bickmeyer, I., and Kuhnlein, R.P. (2011). Reliable Drosophila body fat quantification by a coupled colorimetric assay. PloS one 6, e23796.

Horton, J.D., Shah, N.A., Warrington, J.A., Anderson, N.N., Park, S.W., Brown, M.S., and Goldstein, J.L. (2003). Combined analysis of oligonucleotide microarray data from transgenic and knockout mice identifies direct SREBP target genes. Proceedings of the National Academy of Sciences of the United States of America 100, 12027-12032.

Jiang, H., and Edgar, B.A. (2012). Intestinal stem cell function in Drosophila and mice. Current opinion in genetics & development 22, 354-360.

Jindra, M., Palli, S.R., and Riddiford, L.M. (2013). The juvenile hormone signaling pathway in insect development. Annual review of entomology 58, 181-204.

Jowett, T., and Postlethwait, J.H. (1980). The Regulation of yolk polypeptide synthesis in Drosophila ovaries and fat body by 20-hydroxyecdysone and a juvenile hormone analog. Developmental biology 80, 225-234.

Keller, J., Frederking, D., and Layer, P. (2008). The spectrum and treatment of gastrointestinal disorders during pregnancy. Nature clinical practice. Gastroenterology & hepatology 5, 430-443.

Klepsatel, P., Galikova, M., De Maio, N., Ricci, S., Schlotterer, C., and Flatt, T. (2013). Reproductive and post-reproductive life history of wild-caught Drosophila melanogaster under laboratory conditions. Journal of evolutionary biology 26, 1508-1520.

Koren, O., Goodrich, J.K., Cullender, T.C., Spor, A., Laitinen, K., Backhed, H.K., Gonzalez, A., Werner, J.J., Angenent, L.T., Knight, R., Backhed, F., Isolauri, E., Salminen, S., and Ley, R.E. (2012). Host remodeling of the gut microbiome and metabolic changes during pregnancy. Cell 150, 470-480.

Koyama, T., Mendes, C.C., and Mirth, C.K. (2013). Mechanisms regulating nutrition-dependent developmental plasticity through organ-specific effects in insects. Frontiers in physiology 4, 263.

Kubli, E. (2003). Sex-peptides: seminal peptides of the Drosophila male. Cellular and molecular life sciences : CMLS 60, 1689-1704.

Kunte, A.S., Matthews, K.A., and Rawson, R.B. (2006). Fatty acid auxotrophy in Drosophila larvae lacking SREBP. Cell metabolism 3, 439-448.

Langevin, J., Le Borgne, R., Rosenfeld, F., Gho, M., Schweisguth, F., and Bellaiche, Y. (2005). Lethal giant larvae controls the localization of notch-signaling regulators numb, neuralized, and Sanpodo in Drosophila sensory-organ precursor cells. Current biology : CB 15, 955-962.

Lee, T., and Luo, L. (1999). Mosaic analysis with a repressible cell marker for studies of gene function in neuronal morphogenesis. Neuron 22, 451-461.

Lemaitre, B., and Miguel-Aliaga, I. (2013). The digestive tract of Drosophila melanogaster. Annual review of genetics 47, 377-404.

Li, M., Mead, E.A., and Zhu, J. (2011). Heterodimer of two bHLH-PAS proteins mediates juvenile hormone-induced gene expression. Proceedings of the National Academy of Sciences of the United States of America 108, 638-643.

Lodhi, I.J., Wei, X., and Semenkovich, C.F. (2011). Lipoexpediency: de novo lipogenesis as a metabolic signal transmitter. Trends in endocrinology and metabolism: TEM 22, 1-8.

Marianes, A., and Spradling, A.C. (2013). Physiological and stem cell compartmentalization within the Drosophila midgut. eLife 2, e00886.

Marois, E., and Eaton, S. (2007). RNAi in the Hedgehog signaling pathway: pFRiPE, a vector for temporally and spatially controlled RNAi in Drosophila. Methods in molecular biology 397, 115-128.

McGuire, S.E., Le, P.T., Osborn, A.J., Matsumoto, K., and Davis, R.L. (2003). Spatiotemporal rescue of memory dysfunction in Drosophila. Science 302, 1765-1768.

Micchelli, C.A., and Perrimon, N. (2006). Evidence that stem cells reside in the adult Drosophila midgut epithelium. Nature 439, 475-479.

Middleton, W.R. (1971). Thyroid hormones and the gut. Gut 12, 172-177.

Min, K.T., and Benzer, S. (1999). Preventing neurodegeneration in the Drosophila mutant bubblegum. Science 284, 1985-1988.

Mirth, C.K., and Shingleton, A.W. (2012). Integrating body and organ size in Drosophila: recent advances and outstanding problems. Frontiers in endocrinology 3, 49.

Mirth, C.K., Tang, H.Y., Makohon-Moore, S.C., Salhadar, S., Gokhale, R.H., Warner, R.D., Koyama, T., Riddiford, L.M., and Shingleton, A.W. (2014). Juvenile hormone regulates body size and perturbs insulin signaling in Drosophila. Proceedings of the National Academy of Sciences of the United States of America 111, 7018-7023.

Moshitzky, P., Fleischmann, I., Chaimov, N., Saudan, P., Klauser, S., Kubli, E., and Applebaum, S.W. (1996). Sex-peptide activates juvenile hormone biosynthesis in the Drosophila melanogaster corpus allatum. Archives of insect biochemistry and physiology 32, 363-374.

Navare, A.T., Mayoral, J.G., Nouzova, M., Noriega, F.G., and Fernandez, F.M. (2010). Rapid direct analysis in real time (DART) mass spectrometric detection of juvenile hormone III and its terpene precursors. Analytical and bioanalytical chemistry 398, 3005-3013.

Nijhout, M.M., and Riddiford, L.M. (1974). The control of egg maturation by juvenile hormone in the tobacco hornworm moth, Manduca sexta. The Biological bulletin 146, 377-392.

O'Brien, L.E., Soliman, S.S., Li, X., and Bilder, D. (2011). Altered modes of stem cell division drive adaptive intestinal growth. Cell 147, 603-614.

Padmanabha, D., and Baker, K.D. (2014). Drosophila gains traction as a repurposed tool to investigate metabolism. Trends in endocrinology and metabolism: TEM 25, 518-527.

Palm, W., Sampaio, J.L., Brankatschk, M., Carvalho, M., Mahmoud, A., Shevchenko, A., and Eaton, S. (2012). Lipoproteins in Drosophila melanogaster--assembly, function, and influence on tissue lipid composition. PLoS genetics 8, e1002828.

Parker, L., Gross, S., Beullens, M., Bollen, M., Bennett, D., and Alphey, L. (2002). Functional interaction between nuclear inhibitor of protein phosphatase type 1 (NIPP1) and protein phosphatase type 1 (PP1) in Drosophila: consequences of over-expression of NIPP1 in flies and suppression by co-expression of PP1. The Biochemical journal 368, 789-797.

Parra-Peralbo, E., and Culi, J. (2011). Drosophila lipophorin receptors mediate the uptake of neutral lipids in oocytes and imaginal disc cells by an endocytosis-independent mechanism. PLoS genetics 7, e1001297.

Phillips, M.D., and Thomas, G.H. (2006). Brush border spectrin is required for early endosome recycling in Drosophila. Journal of cell science 119, 1361-1370.

Piersma, T., and Lindstrom, A. (1997). Rapid reversible changes in organ size as a component of adaptive behaviour. Trends in ecology & evolution 12, 134-138.

Rauschenbach, I.Y., Karpova, E.K., Adonyeva, N.V., Andreenkova, O.V., Faddeeva, N.V., Burdina, E.V., Alekseev, A.A., Menshanov, P.N., and Gruntenko, N.E. (2014). Disruption of insulin signalling affects the neuroendocrine stress reaction in Drosophila females. The Journal of experimental biology 217, 3733-3741.

Rera, M., Bahadorani, S., Cho, J., Koehler, C.L., Ulgherait, M., Hur, J.H., Ansari, W.S., Lo, T., Jr., Jones, D.L., and Walker, D.W. (2011). Modulation of longevity and tissue homeostasis by the Drosophila PGC-1 homolog. Cell metabolism 14, 623-634.

Riddiford, L.M. (2012). How does juvenile hormone control insect metamorphosis and reproduction? General and comparative endocrinology 179, 477-484.

Roa, J., and Tena-Sempere, M. (2014). Connecting metabolism and reproduction: Roles of central energy sensors and key molecular mediators. Molecular and cellular endocrinology.

Rogina, B., Wolverton, T., Bross, T.G., Chen, K., Muller, H.G., and Carey, J.R. (2007). Distinct biological epochs in the reproductive life of female Drosophila melanogaster. Mechanisms of ageing and development 128, 477-485.

Ryu, J.H., Kim, S.H., Lee, H.Y., Bai, J.Y., Nam, Y.D., Bae, J.W., Lee, D.G., Shin, S.C., Ha, E.M., and Lee, W.J. (2008). Innate immune homeostasis by the homeobox gene caudal and commensal-gut mutualism in Drosophila. Science 319, 777-782.

Sarraf-Zadeh, L., Christen, S., Sauer, U., Cognigni, P., Miguel-Aliaga, I., Stocker, H., Kohler, K., and Hafen, E. (2013). Local requirement of the Drosophila insulin binding protein imp-L2 in coordinating developmental progression with nutritional conditions. Developmental biology 381, 97-106.

Schneider, C.A., Rasband, W.S., and Eliceiri, K.W. (2012). NIH Image to ImageJ: 25 years of image analysis. Nature methods 9, 671-675.

Seegmiller, A.C., Dobrosotskaya, I., Goldstein, J.L., Ho, Y.K., Brown, M.S., and Rawson, R.B. (2002). The SREBP pathway in Drosophila: regulation by palmitate, not sterols. Developmental cell 2, 229-238.

Shimano, H. (2001). Sterol regulatory element-binding proteins (SREBPs): transcriptional regulators of lipid synthetic genes. Progress in lipid research 40, 439-452.

Shin, S.W., Zou, Z., Saha, T.T., and Raikhel, A.S. (2012). bHLH-PAS heterodimer of methoprene-tolerant and Cycle mediates circadian expression of juvenile hormone-induced mosquito genes. Proceedings of the National Academy of Sciences of the United States of America 109, 16576-16581.

Sieber, M.H., and Thummel, C.S. (2012). Coordination of triacylglycerol and cholesterol homeostasis by DHR96 and the Drosophila LipA homolog magro. Cell metabolism 15, 122-127.

Siegmund, T., and Korge, G. (2001). Innervation of the ring gland of Drosophila melanogaster. The Journal of comparative neurology 431, 481-491.

Song, W., Veenstra, J.A., and Perrimon, N. (2014). Control of lipid metabolism by tachykinin in Drosophila. Cell reports 9, 40-47.

Speakman, J.R. (2008). The physiological costs of reproduction in small mammals. Philosophical transactions of the Royal Society of London. Series B, Biological sciences 363, 375-398.

R Development Core Team. (2014). R: a language and environment for statistical Computing. (R Foundation for Statistical Computing).

Theopold, U., Ekengren, S., and Hultmark, D. (1996). HLH106, a Drosophila transcription factor with similarity to the vertebrate sterol responsive element binding protein. Proceedings of the National Academy of Sciences of the United States of America 93, 1195-1199.

Tiu, S.H., Hult, E.F., Yagi, K.J., and Tobe, S.S. (2012). Farnesoic acid and methyl farnesoate production during lobster reproduction: possible functional correlation with retinoid X receptor expression. General and comparative endocrinology 175, 259-269.

Ueyama, M., and Fuyama, Y. (2003). Enhanced cost of mating in female sterile mutants of Drosophila melanogaster. Genes & genetic systems 78, 29-36.

Venables, W.N., and Ripley, B.D. (2002). Modern applied statistics with S. (New York: Springer).

Wen, D., Rivera-Perez, C., Abdou, M., Jia, Q., He, Q., Liu, X., Zyaan, O., Xu, J., Bendena, W.G., Tobe, S.S., Noriega, F.G., Palli, S.R., Wang, J., and Li, S. (2015). Methyl farnesoate plays a dual role in regulating Drosophila metamorphosis. PLoS genetics 11, e1005038.

Wigby, S., and Chapman, T. (2005). Sex peptide causes mating costs in female Drosophila melanogaster. Current biology : CB 15, 316-321.

Wyatt, G.R., and Davey, K.G. (1996). Cellular and molecular actions of juvenile hormone. II. Roles of juvenile hormone in adult insects. Advances in Insect Physiology 26, 1-155.

Yamamoto, R., Bai, H., Dolezal, A.G., Amdam, G., and Tatar, M. (2013). Juvenile hormone regulation of Drosophila aging. BMC biology 11, 85.

Yin, C., Zou, B., Jiang, M., Li, M., Qin, W., Potter, T.L., and Stoffolano, J.G. (1995). Identification of juvenile hormone III bisepoxide (JHB3), juvenile hormone III and methyl farnesoate secreted by the corpus allatum of Phormia regina (Meigen), in vitro and function of JHB3 either applied alone or as a part of a juvenoid blend. Journal of insect physiology 41, 473-479.

Zhang, Z., Xu, J., Sheng, Z., Sui, Y., and Palli, S.R. (2011). Steroid receptor co-activator is required for juvenile hormone signal transduction through a bHLH-PAS transcription factor, methoprene tolerant. The Journal of biological chemistry 286, 8437-8447.

Figure 1

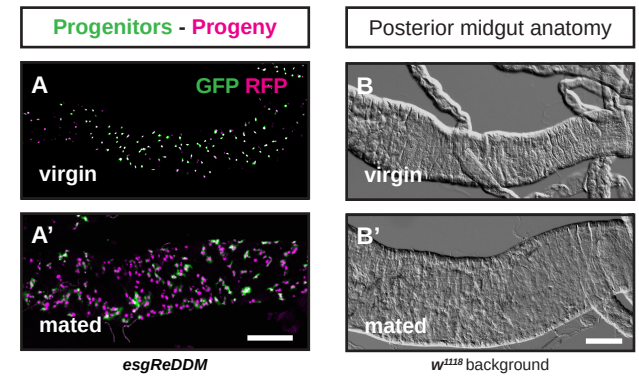
Progenitors - Progeny
Posterior midgut anatomy
A
GFP RFP
virgin
A'
mated
B
virgin
B'
mated
esgReDDM
w1118 background

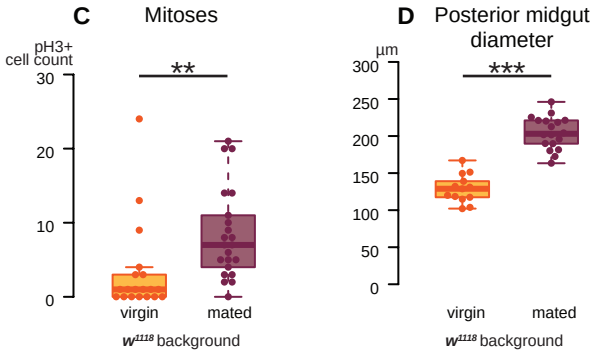
C
Mitoses
pH3+ cell count
30
20
10
0
**
virgin
mated
w1118 background
D
Posterior midgut diameter
µm
300
250
200
150
100
50
0
***
virgin
mated
w1118 background

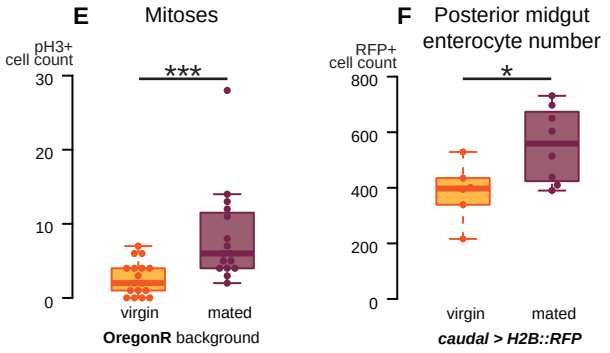
E
Mitoses
pH3+ cell count
30
20
10
0
***
virgin
mated
OregonR background
F
Posterior midgut enterocyte number
RFP+ cell count
800
600
400
200
0
*
virgin
mated
caudal > H2B::RFP

Figure 1 - Supplement 1

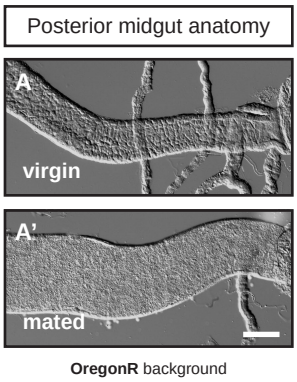

OregonR background

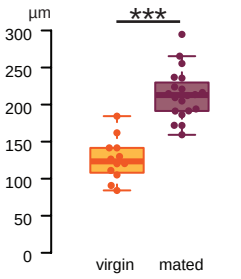

OregonR background

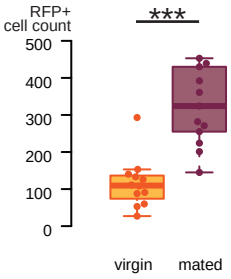

esgReDDM

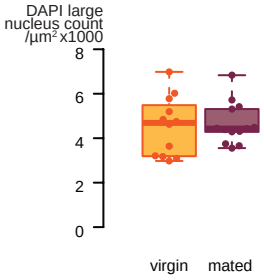

esgReDDM

Figure 2

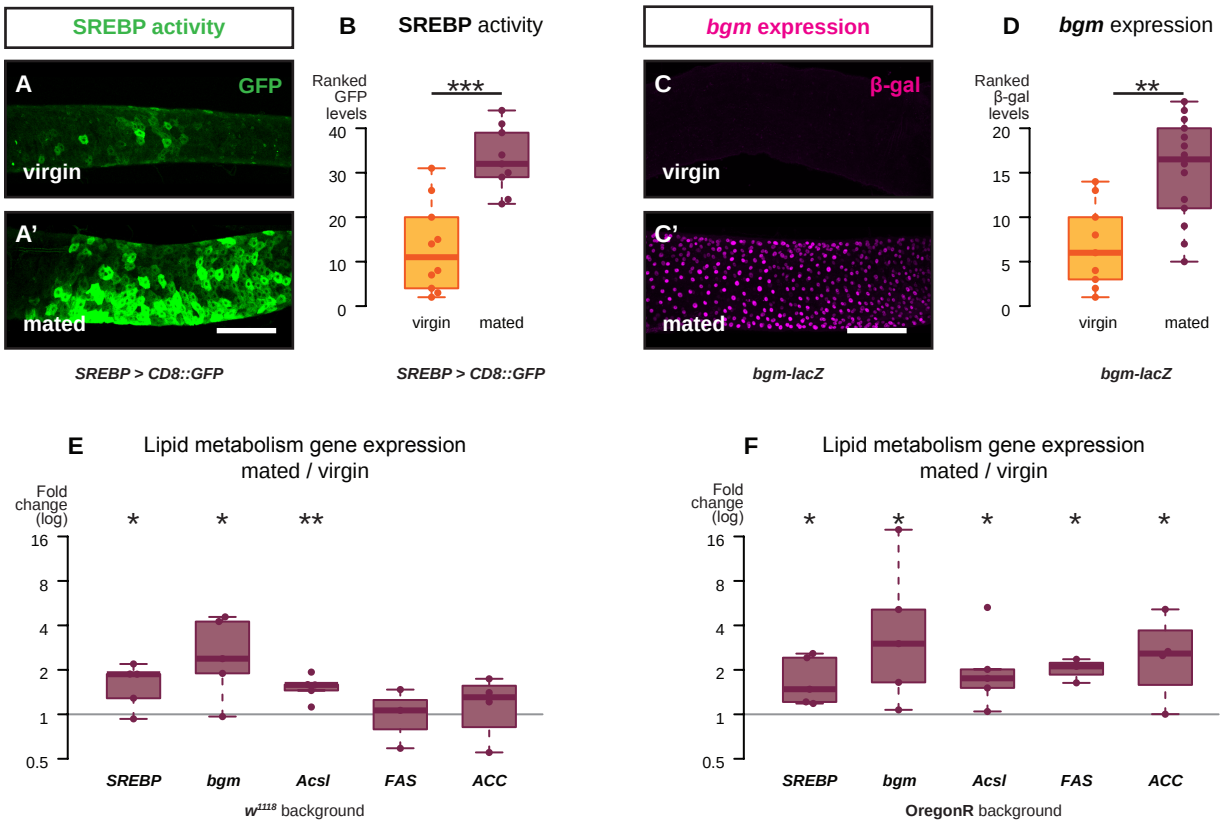
SREBP activity
A
GFP
virgin
A'
mated
SREBP > CD8::GFP
B
SREBP activity
Ranked GFP levels
40
30
20
10
0
***
virgin
mated
SREBP > CD8::GFP
bgm expression
C
β-gal
virgin
C'
mated
bgm-lacZ
D
bgm expression
Ranked β-gal levels
20
15
10
5
0
**
virgin
mated
bgm-lacZ
E
Lipid metabolism gene expression
mated / virgin
Fold change (log)
16
8
4
2
1
0.5
* * **
SREBP
bgm
AcsI
FAS
ACC
w1118 background
F
Lipid metabolism gene expression
mated / virgin
Fold change (log)
16
8
4
2
1
0.5
* * * * *
SREBP
bgm
AcsI
FAS
ACC
OregonR background

Figure 3

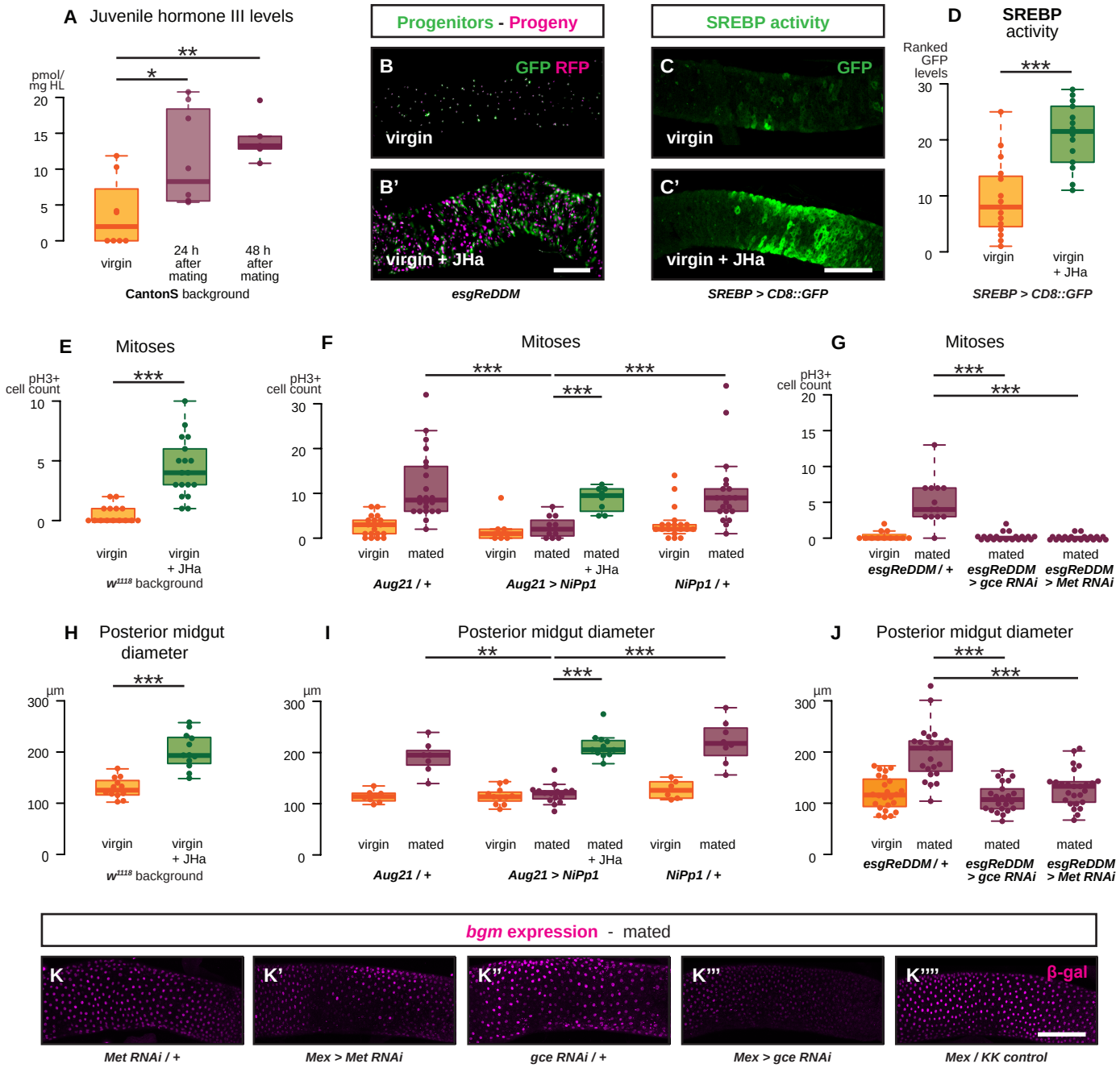
A Juvenile hormone III levels
pmol/ mg HL
virgin
24 h after mating
48 h after mating
CantonS background
Progenitors - Progeny
B GFP RFP
virgin
B'
virgin + JHa
esgReDDM
SREBP activity
C GFP
virgin
C'
virgin + JHa
SREBP > CD8::GFP
D SREBP activity
Ranked GFP levels
virgin
virgin + JHa
SREBP > CD8::GFP
E Mitoses
pH3+ cell count
virgin
virgin + JHa
w1118 background
F Mitoses
pH3+ cell count
virgin
mated
mated + JHa
Aug21 / +
Aug21 > NiPp1
NiPp1 / +
G Mitoses
pH3+ cell count
esgReDDM / +
esgReDDM > gce RNAi
esgReDDM > Met RNAi
H Posterior midgut diameter
µm
w1118 background
I Posterior midgut diameter
µm
Aug21 / +
Aug21 > NiPp1
NiPp1 / +
J Posterior midgut diameter
µm
esgReDDM / +
esgReDDM > gce RNAi
esgReDDM > Met RNAi
bgm expression - mated
K
Met RNAi / +
K'
Mex > Met RNAi
K''
gce RNAi / +
K'''
Mex > gce RNAi
K''''
β-gal
Mex / KK control

Figure 3 - Supplement 1

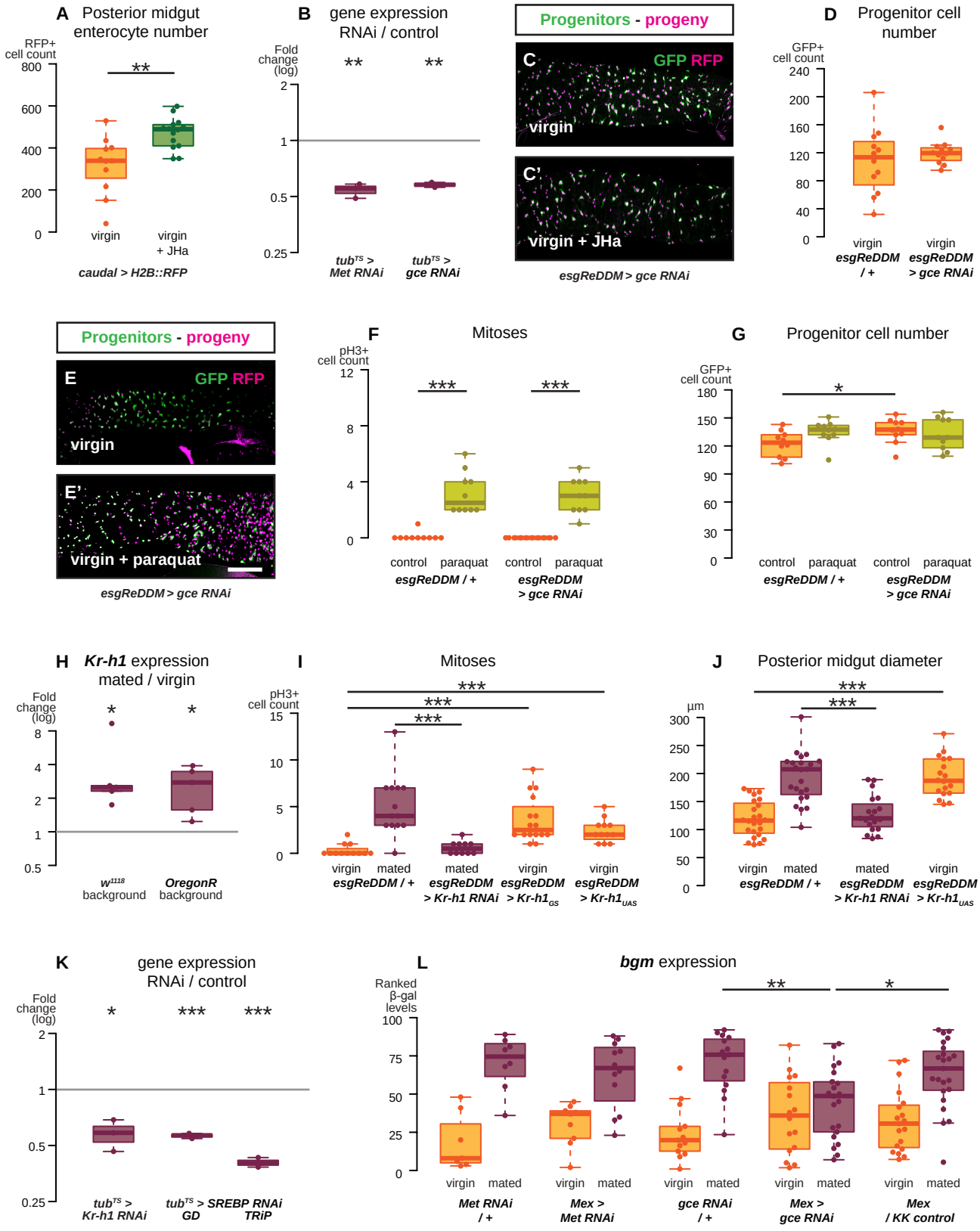

Figure 4

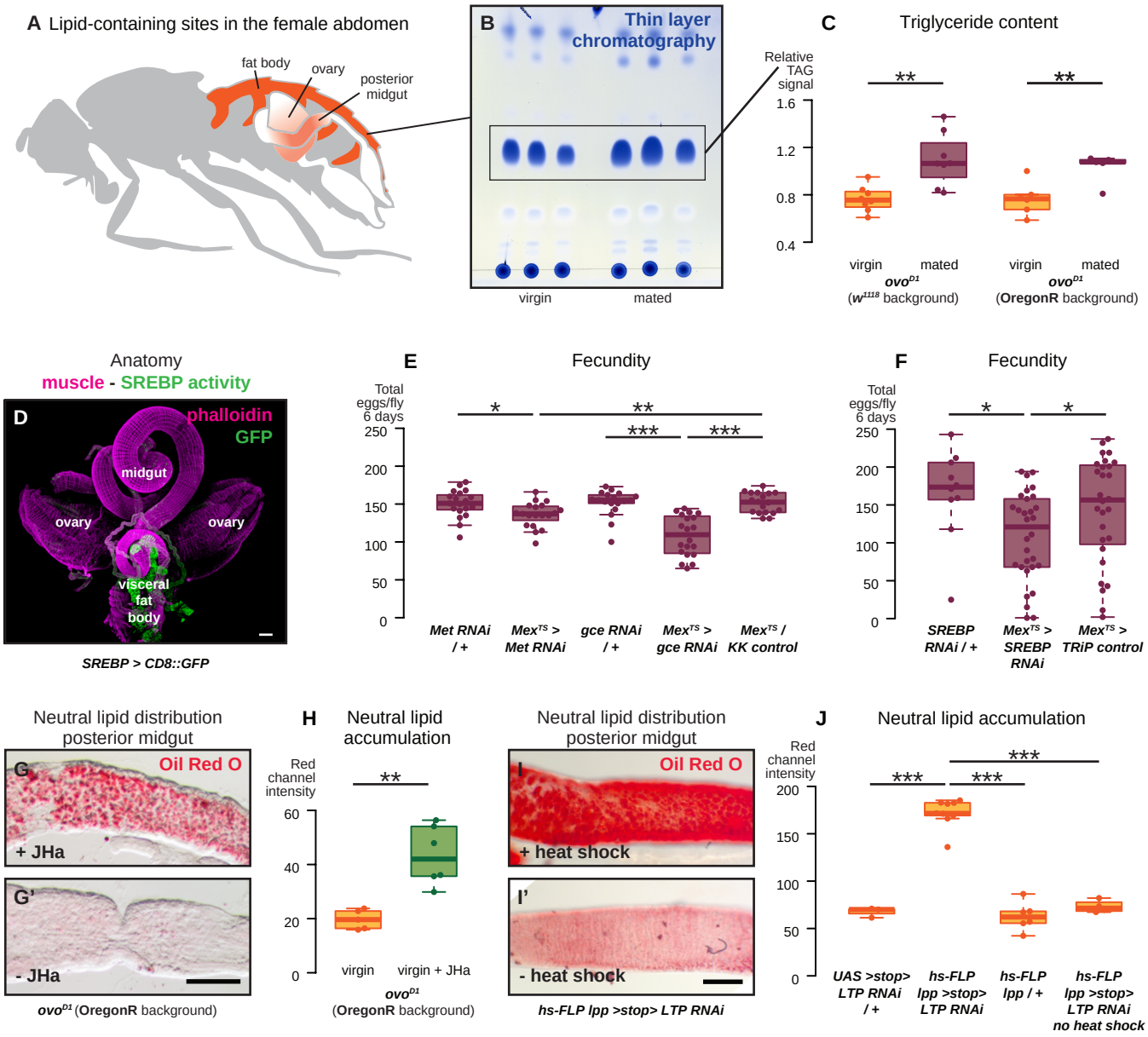
A Lipid-containing sites in the female abdomen
fat body
ovary
posterior midgut
B
Thin layer chromatography
virgin
mated
C
Triglyceride content
Relative TAG signal
1.6
1.2
0.8
0.4
**
**
virgin
mated
ovoD1 (w1118 background)
virgin
mated
ovoD1 (OregonR background)
Anatomy
muscle - SREBP activity
D
phalloidin
GFP
midgut
ovary
ovary
visceral fat body
SREBP > CD8::GFP
E
Fecundity
Total eggs/fly 6 days
250
200
150
100
50
0
*
**
***
***
Met RNAi / +
MexTS > Met RNAi
gce RNAi / +
MexTS > gce RNAi
MexTS / KK control
F
Fecundity
Total eggs/fly 6 days
250
200
150
100
50
0
*
*
SREBP RNAi / +
MexTS > SREBP RNAi
MexTS > TRiP control
Neutral lipid distribution posterior midgut
G
Oil Red O
+ JHa
G'
- JHa
ovoD1 (OregonR background)
H
Neutral lipid accumulation
Red channel intensity
60
40
20
0
**
virgin
virgin + JHa
ovoD1 (OregonR background)
Neutral lipid distribution posterior midgut
I
Oil Red O
+ heat shock
I'
- heat shock
hs-FLP lpp >stop> LTP RNAi
J
Neutral lipid accumulation
Red channel intensity
200
150
100
50
0
***
***
***
UAS >stop> LTP RNAi / +
hs-FLP lpp >stop> LTP RNAi
hs-FLP lpp / +
hs-FLP lpp >stop> LTP RNAi no heat shock

Figure 4 - Supplement 1